Molecular characteristics of single patient-derived glioma stem-like cells from primary and recurrent glioblastoma

Jia Shi[a,b]*, Xuchen Dong[a]*, Wei Han[c]*, Peng Zhou[b], Liang Liu[a], Haiyang Wang[a], Qianqian Jiang[a], Haoran Li[a], Shan Cheng[a], Suwen Li[a], Jiaqi Yuan[a], Zhiyuan Qian[a] and Jun Dong[a]

Glioblastoma has high recurrence, while the sensitivity of recurrent glioblastoma to chemotherapy is lower than that of primary glioblastoma. Moreover, there is no standardized treatment for recurrent glioblastoma. Unfortunately, the biological mechanism of recurrent glioblastoma is still unclear, and there are few related studies. We compared the phenotypes of clinical glioblastoma specimens, in-vitro cultured glioma stem-like cells (GSCs) and patient-derived xenograft tumor (PDX) models to explore the molecular genetic characteristics of primary and recurrent glioblastoma from the same patient. *In vitro*, SU5-2, GSCs derived from recurrent glioblastoma specimens, had stronger proliferative activity and self-renewal ability. Meanwhile, SU5-2 was more resistant to temozolomide and invasive than SU5-1, which derived from primary glioblastoma specimens. Further analysis of the expression of costimulatory molecules showed that the expression of B7-H1, B7-H2 and B7-H3 of SU5-2 were upregulated. In vivo, Kaplan–Meier survival curve analysis showed that the median survival of the recurrent PDX group was worse. The results of gene detection *in vitro*, PDX model and clinical samples were consistent. Our results showed that the GSCs based on glioblastoma specimens and the PDX models could replicate the main molecular genetic characteristics of original tumors, which provided a reliable experimental platform for both tumor translation kinds of research and screening of molecular therapeutic targets. *Anti-Cancer Drugs* 33: e381–e388

Anti-Cancer Drugs 2022, **33**:e381–e388

Keywords: glioblastoma, patient-derived xenograft tumor model, glioma stem cells, recurrence

[a]Department of Neurosurgery, The Second Affiliated Hospital of Soochow University, Suzhou, [b]Department of Neurosurgery, The Third Affiliated Hospital of Soochow University, Changzhou and [c]Department of Clinical Medical Research Center, The Third Affiliated Hospital of Soochow University, Changzhou, China

Correspondence to Jun Dong, Department of Neurosurgery, The Second Affiliated Hospital of Soochow University, No. 1055, Sanxiang Street, Suzhou, Jiangsu 215004, China
Tel/fax: +86 0512 67784089; e-mail: dongjun@suda.edu.cn

*Jia Shi, Xuchen Dong, and Wei Han contributed equally to the writing of this article.

Received 22 April 2021 **Revised form accepted** 14 July 2021

Introduction

Glioblastoma is the most common and invasive malignant tumor in the central nervous system. Its 5-year survival rate is less than 10% [1]. Though small molecular targeted drugs related to tumor treatment have existed in recent years [2], the inner mechanism of occurrence, progression, and recurrence of glioblastoma is still far from definite and needs further exploration. There is still an urgent need for drug detection platforms that can accurately reflect the cytogenetics and molecular characteristics for glioblastoma *in vitro* and *in vivo*. However, the classic glioma cell lines such as U87MG and U251, widely used in tumor mechanism researches, have accumulated molecular mutations unrelated to the genetic characteristics of the original gene during the long-term culture *in vitro* [3]. The U87MG human glioma cell retained by the American Type Culture Collection has lost the main molecular genetic characteristics of the original glioma [4]. Therefore, it is important to establish primary tumor cells which can accurately reflect the original tumor molecules. Glioma stem-like cells (GSCs) have self-renewal, proliferation, multi-differentiation potential and tumorigenicity, which are related to the resistance of glioblastoma to chemotherapy and radiotherapy [5], leading to the progression and recurrence of glioblastoma [6]. In addition, the technology of the patient-derived xenograft (PDX) model provides a reliable and effective platform for preclinical drug efficacy evaluation. Compared with the tumor model established by cell line, the PDX model reduces the culture procedure *in vitro* and retains tumor stromal components, namely tumor microenvironment, which is in line with the morphological and molecular biological characteristics of clinical tumor tissue and is a better clinical simulation model.

In this study, a case of glioblastoma with spontaneous recurrence without the interference of radiochemotherapy-induced hyperprogression was studied. We not only established PDX model, but also established GSCs in primary culture to compare the molecular genetic

0959-4973 Copyright © 2021 The Author(s). Published by Wolters Kluwer Health, Inc. DOI: 10.1097/CAD.0000000000001217

characteristics among original glioblastoma specimens, GSCs *in vitro* and PDX models, so as to lay a foundation for further transformation research.

Methods

Clinical sample

A 32-year-old man was admitted to the hospital with a headache. MRI showed a left-frontal lesion with a strengthening effect (5.1×4.0 cm), and the symptoms disappeared after complete tumor resection. The postoperative pathology was glioblastoma. After the operation, the patient refused chemoradiotherapy and routine follow-up. Half a year later, the headache recurred and MRI showed the tumor recurred *in situ* (4.8×4.2 cm). In the second operation, the previous approach was used, and the postoperative pathology was still glioblastoma. The patient refused chemoradiotherapy again and died 9 months later. Tumor specimens were collected during the operations. *IDH* and *PDGFRα* mutation was detected by PCR sequencing, *MGMT* methylation was carried out by methylation-specific PCR, *Pten* mutation was analyzed by immunohistochemical staining and *EGFR* amplification was detected by fluorescent in-situ hybridization (*EGFR* detection meets any of the following is positive: *EGFR* scattered signal >4 cells >40%; *EGFR*/*CEP7* signal ratio >2.0; *EGFR* cluster signal >4 cells >10%; *EGFR* scattered signal >15 cells >10%). The study was approved by the ethics committee of the Second Affiliated Hospital of Soochow University.

Reagents and animals

Dulbecco's modified eagle medium, fetal bovine serum (FBS), basic fibroblast growth factor and epidermal growth factor (EGF) were purchased from Gibco, Grand Island, New York, USA. Primary antibodies against CD133, β3-tubulin, Nestin, glial fibrillary acidic protein (GFAP), B7-H1 (PD-L1), B7-H2, B7-H3 and Ki67 were obtained from Cell Signaling Technology, Danvers, Massachusetts, USA or Abcam, Cambridge, UK. Temozolomide and afatinib were purchased from Selleck, Houston, Texas, USA. Three to four weeks Balb/c male nude mice were obtained from the Nanjing Institute of Model Animals (Nanjing, Jiangsu, China).

Cell culture

The primary cultured cells were derived from fresh surgical specimens of human glioblastoma tissues by a method described previously with informed consent [7]. GSCs were seeded in six-well plates under stem cell culture conditions [8]. The differentiation of GSCs was induced by adding 10% FBS into stem cell culture medium.

Cell survival assay

GSCs were cultured in 96-well plates (2×10^3 cells/well) pre-coated with Lamin (Sigma, St. Louis, Missouri, USA) at 10 μg/mL and incubated overnight [9], then were treated with different dosages of temozolomide or afatinib for 72 h. The concentrations of temozolomide applied were as following, 50, 100, 200, 400, 800, and 1600 μM. The concentration of afatinib were 0.01, 0.1, 1.0, 3.0, 10, and 30 μM. Cell counting kit-8 solution (Dojindo, Kumamoto, Japan) was supplemented into each well, incubated for 2 h at 37°C. The absorbance values were measured at 490 nm on a microplate reader EL×800 (BioTek, Winooski, Vermont, USA). The viability of untreated cells was set as 100%. The experiment was repeated three times.

Neurosphere formation assay

GSCs were seeded in 96-well plates (1×10^3 cells per well) with five duplicate wells and supplemented with 50 μL culture medium every 3 days. Neurospheres numbers and diameters were observed under a microscope (Nikon, Tokyo, Japan) after 10 days of incubation.

Flow cytometry analysis

Cells were incubated with fluorescent antibody B7-H1 (PD-L1) for 30 min after fixation and membrane breaking, then centrifuged and resuspended for flow cytometry (Guava EasyCyte 6HT-2L, Merck Millipore, Darmstadt, Germany). The experiment was repeated three times.

Cell invasion assay

Matrigel (BD, Franklin Lake, New Jersey, USA) was diluted with a serum-free medium (1:5) to pretreat the transwell chamber (Corning, Corning, New York, USA). The procedure of GSCs invasion was as described [9]. Each group was repeated three times.

Western blot

Total protein was extracted by radio-immunoprecipitation assay (Beyotime, Shanghai, Jiangsu, China). Protein concentration was determined with a standard BCA Protein Assay Kit (Thermo Fisher Scientific, Waltham, Massachusetts, USA). Western blot procedure was performed according to the standard protocol. Primary antibodies against B7-H1 (PD-L1, #13684; CST, USA), B7-H3 (#14058; CST, USA) and B7-H2 (#ab209262; Abcam). Rabbit anti-β-actin was used as normal loading control. An ECL plus kit (Thermo Fisher Scientific) and a ChemiDoc Touch Imaging System (BioRad, Hercules, California, USA) were applied to detect the chemiluminescence signals. Each experiment was repeated three times.

PDX model

Fresh tumor tissue (2 mm^3) derived from surgical specimens was transplanted to caudate nucleus of 3–4 weeks Balb/c nude mice with a self-made tissue inoculation needle stereotactic instrument [10]. The overall survival (OS) of mice was recorded and analyzed by Kaplan–Meier survival curves. Intracranial transplanted tumors were dissected, fixed by neutral formalin.

Immunohistochemical staining

Immunohistochemical staining was performed as previously described [8]. Diluted Rabbit anti-human primary

Fig. 1

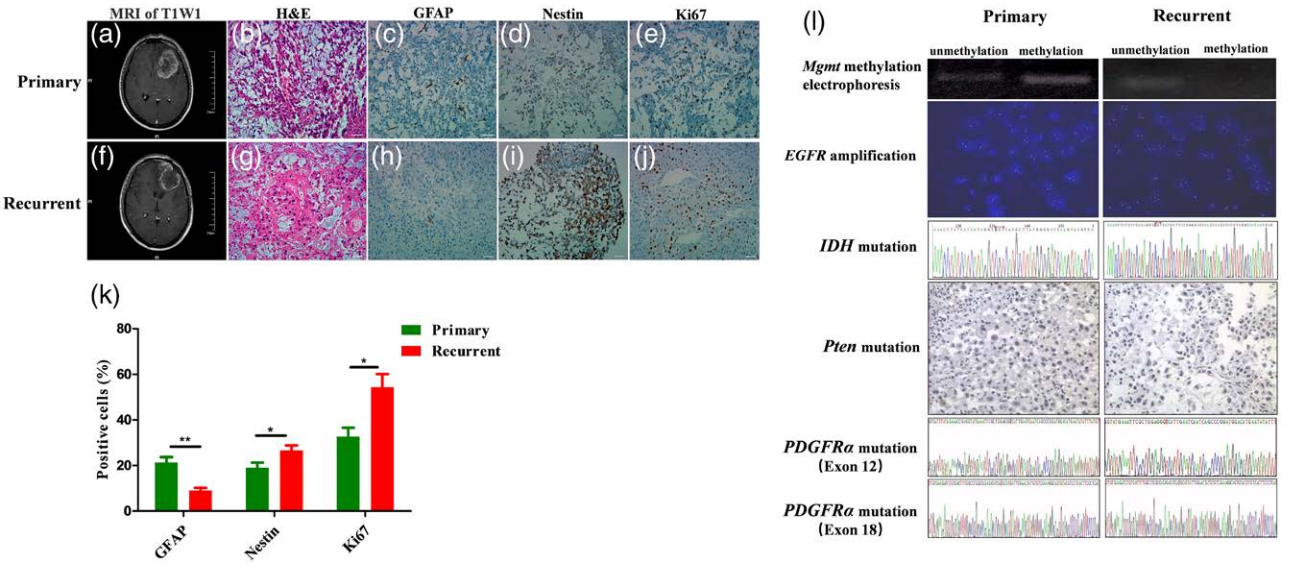

Clinical sample pathological analysis. (a, f) Enhanced MRI of primary and recurrent glioblastoma. (b–e, g–j) H&E staining, immunohistochemical staining of GFAP, Nestin and Ki67 in primary and recurrent glioblastoma sample (×200). (k) Statistical analysis of the positive cells of Ki-67, Nestin and GFAP in primary and recurrent glioblastoma. *$P<0.05$, **$P<0.01$. (l) Gene detection. *IDH* mutation detection by using PCR sequencing method and *MGMT* methylation detection was carried out by methylation-specific PCR. Fluorescent in-situ hybridization technology was used in EGFR amplification detection. GFAP, glial fibrillary acidic protein.

antibody (#ab7260, #ab105389, #ab15580, 1:200) was added and incubated at 4°C overnight after antigen repair and goat serum blocking. Goat anti-rabbit IgG secondary antibody incubated for 1 h. Then, diaminobenzidine staining and hematoxylin re-staining, dehydrated and sealed. Under the microscope, five pictures were taken randomly for each and the positive cells were counted.

Immunofluorescent staining

Cells were fixed with 4% paraformaldehyde for 15 min, permeabilized with 0.5% Triton X-100 for 20 min, blocked with 10% goat serum for 1 h. 10% goat serum was used to prepare the primary antibody (#ab105389, #ab222782, #ab7260, 1:100), incubated overnight at 4°C. Diluted fluorescent antibody incubated for 2 h. A terminal deoxynucleotidyl transferase-mediated dUTP-biotin nick end labeling (TUNEL kit, Roche, Switzerland) assay (TUNEL kit) was applied to detect GSCs apoptosis, and procedures followed the standard protocol. The nuclei were stained with 4,6-diamino-2-phenyl indole. Reviewed and quantified under a fluorescence microscope (Nikon, Kawasaki, Japan).

Statistical analysis

Graphpad 7.0 software was used for data analysis. The *t*-test was used for comparison between the two groups. $P<0.05$ was considered statistically significant.

Results

Clinical sample pathological analysis

MRI showed oval irregular ring enhancement, central necrosis and peritumoral edema in the left frontal lobe (Fig. 1a and f). Both the pathological results were glioblastoma. In H&E morphology, cells of the relapsed specimen had a higher density and more cell atypia. It was easy to find tumor giant cells with higher microvessel density and a wider range of necrosis (Fig. 1b and g). In addition, the expression of GFAP in primary glioblastoma was higher than that in relapsed glioblastoma while Nestin positive cells were more in relapsed glioblastoma (Fig. 1c, d, h, i, k), indicating a higher ratio of tumor stem/initiating cells in recurrent glioblastoma. Ki67, as a sensitive indicator of mitosis, was used to detect cell proliferation. We found that the positive rate of Ki67 in recurrent samples was higher (Fig. 1e, j, k), which meant that the recurrent tumor had stronger proliferative activity. Gene detection analysis showed that *IDH*, *Pten* and *PDGFRα* (*Exon 12* and *18*) genes were not mutated in primary and recurrent glioma tissues, *MGMT* in primary gliomas was methylated, *EGFR* was not amplified, while *MGMT*

Table 1 Detection of genes related to primary and recurrent glioblastoma, glioma stem-like cells *in vitro*, and patient-derived xenograft tumor models

Samples	Methylation of *MGMT*	*IDH* mutation	*Pten* mutation	*PDGFRα* mutation	*EGFR* amplification
Primary clinical specimen	+	−	−	−	−
Recurrent clinical specimens	−	−	−	−	+
SU5-1	+	−	−	−	−
SU5-2	−	−	−	−	+
Primary PDX	+	−	−	−	−
Recurrent PDX	−	−	−	−	+

PDX, patient-derived xenograft tumor.

in relapsed glioblastoma was unmethylated and *EGFR* amplification was positive (Table 1 and Fig. 1l).

SU5-2 showed stronger self-renew and proliferative activity *in vitro*

We established GSCs named SU5-1 and SU5-2 by cell culture of primary and recurrent tumor samples. The experimental methods refer to our previous report [7]. Both GSCs lines are characterized by neurospheres and expressed stem/progenitor cell markers Nestin and CD133 (Fig. 2a–c and g–i). Subsequently, GSCs were induced to differentiate with 10% FBS, the cells showed adherent growth, pseudopodia and diverse morphology (Fig. 2d and j). In order to assess the differentiation of SU5-1 and SU5-2, we performed immunofluorescence to verify the expression of GFAP and tubulin, which are markers of glial and neurons lineage, respectively (Fig. 2e, f, k and l).

In order to demonstrate the self-renewal ability and proliferation ability of SU5-1 and SU5-2 *in vitro*, we carried out a neurosphere formation assay and cell viability assay. By quantifying the number of neurospheres under different cell density gradients, we found that SU5-2 had more neurospheres at the same cell concentration (Fig. 2m). Simultaneously, we measured the diameter of the neurospheres of both cells, the average diameter of the neurospheres formed by SU5-2 was larger than that of SU5-1 (Fig. 2n). These results indicated that SU5-2 had stronger self-renewal ability *in vitro*. In the cell viability assay, SU5-2 also showed stronger proliferation activity (Fig. 2o).

SU5-2 showed stronger chemoresistance and invasiveness *in vitro*

Temozolomide is the chemotherapy in the standard treatment protocol (STUPP) for glioblastoma [11]. We applied different concentrations of temozolomide to SU5-1 and SU5-2, and found that these two GSCs were resistant to temozolomide, but only inhibited by high concentration of temozolomide (Fig. 3a), which was consistent with previous reports [12]. Comparing the proliferation ability of the two GSCs lines at the concentration of 400, 800, 1600 μM of temozolomide, temozolomide inhibited SU5-1 more than SU5-2 (Fig. 3a). For further verification, TUNEL assay was performed at the concentration of 400 μM of temozolomide, and the result revealed that the apoptosis of SU5-1 was more obvious (Fig. 3b).

Similarly, we compared the self-renewal ability of SU5-1 and SU5-2 under temozolomide. With the increasing concentration of temozolomide, the number and diameter of

Fig. 2

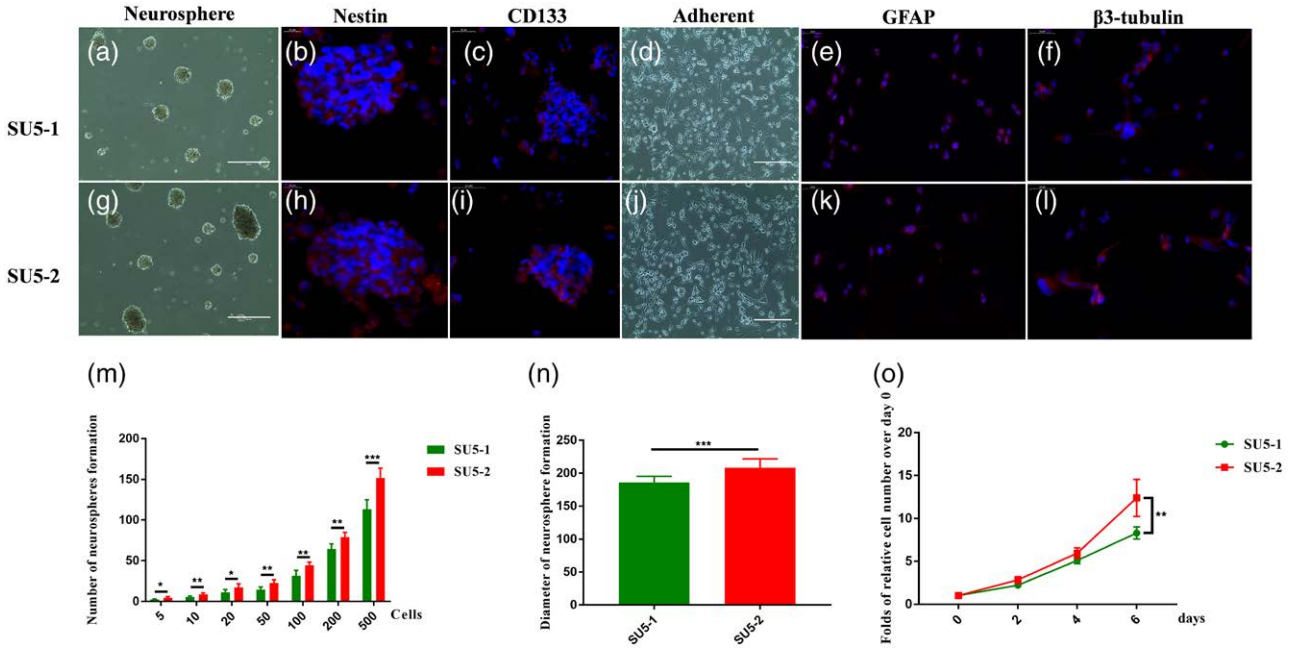

SU5-2 showed stronger self-renew and proliferative activity *in vitro*. (a, g) Under the phase-contrast microscope, SU5-1 and SU5-2 showed spherical growth (Scale bar 400 μM). (b, c, h, i) CD133 and Nestin were positively expressed in SU5-1 and SU5-2, determined by immunofluorescence staining (b, h scale bar 20 μM. c, I scale bar 50 μM). (d, j) Briefly cultured SU5-1 and SU5-2 after differentiation with 10% FCS (Scale bar 400 μM). (e, f, k, l) GFAP and β3-tubulin were positively expressed after differentiation, determined by immunofluorescence staining (Scale bar 50 μM). (m, n) The quantification of numbers and diameter of SU5-1 and SU5-2 neurospheres showing that the neurosphere formation ability of SU5-2 was stronger. **P*<0.05, ***P*<0.01, ****P*<0.001. (o) The proliferation activity of SU5-1 and SU5-2 was measured by CCK8 assay. **P*<0.05, ***P*<0.01, ****P*<0.001. CCK8, cell counting kit-8; GFAP, glial fibrillary acidic protein.

Fig. 3

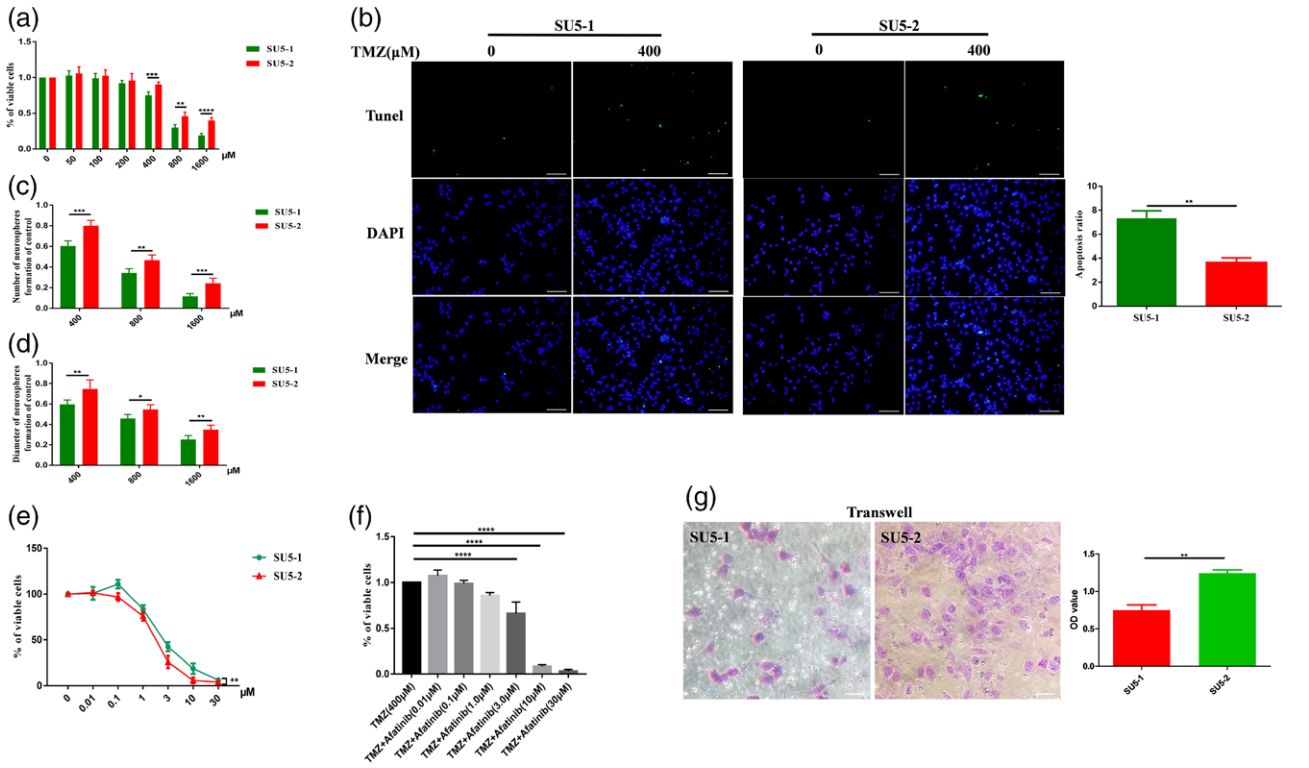

SU5-2 showed stronger chemoresistance and invasiveness *in vitro*. (a) Cell survival assay by CCK-8 after administering temozolomide ranging from 0 to 1600 μM for 72 h. (b) SU5-1 and SU5-2 were exposed to temozolomide (400 μM) for 72 h and detected by TUNEL assay. (c, d) The quantification of numbers and diameter of SU5-1 and SU5-2 after administering temozolomide ranging from 400 to 1600 μM for 72 h. (e) Cell survival assay by CCK-8 after administering afatinib ranging from 0 to 30 μM for 72 h. (f) Cell survival assay by CCK-8 after administering temozolomide (400 μM) combined with afatinb (0.01, 0.1, 1, 3, 10, 30 μM) for 72 h. (g) Invasion ability was determined in SU5-1 and SU5-2 by a transwell assay. CCK-8, cell counting kit-8. **P*<0.05, ***P*<0.01, ****P*<0.001, *****P*<0.0001.

neurospheres in SU5-1 and SU5-2 decreased, which was more apparent in SU5-1 (Fig. 3c and d). These results implied that SU5-2 from recurrent tumor specimens showed stronger resistance to temozolomide *in vitro*.

Afatinib and neratinib are dual inhibitors of epidermal growth factor receptor (EGFR) and human epidermal growth factor receptor-2 tyrosine kinase, which can be used alone or as adjuvants in chemotherapy, especially for $EGFR^+$ cells [13]. In order to verify the efficacy, we detected the sensitivity of afatinib to SU5-1 and SU5-2 in different concentration gradients. The results showed that afatinib had a stronger inhibitory effect on SU5-2, which was EGFR positive (Fig. 3e). Immediately, we treated SU5-2 with temozolomide combined with different concentrations of afatinib. Cell viability assay showed that low concentration (<3 μM) of afatinib could not enhance the cytotoxicity of temozolomide, while high concentration (>10 μM) of afatinib combined with temozolomide significantly enhanced the inhibition of SU5-2. According to previous studies, the dose of afatinib in combination with other chemotherapeutics was in the range of 0.5–1 μM [14–16]. Considering that a high concentration of afatinib itself had a toxic effect on EGFR+ cells, the enhanced inhibitory effect after combination was more likely to be the superposition of chemotherapy agents, rather than the sensitization effect of afatinib on temozolomide (Fig. 3f).

High invasiveness promotes the progression and recurrence of glioblastoma [9]. Therefore, we explored the invasive properties of SU5-1 and SU5-2 *in vitro* by transwell assay which showed that the SU5-2 was more invasive than that of SU5-1 (Fig. 3g).

Upregulation of PD-L1 expression in SU5-2

The expression of PD-L1 in glioblastoma was about 40% [17]. Meta-analysis showed the expression of PD-L1 was negatively correlated with the OS of glioblastoma, and high expression of PD-L1 was a biomarker of glioblastoma progression and poor prognosis [1]. In order to determine the expression of PD-L1 in SU5-1 and SU5-2, Western blot and flow cytometry were performed. Results showed that the expression of B7-H1 (PD-L1), B7-H2 and B7-H3 in SU5-2 which derived from recurrent glioblastoma was upregulated than that in SU5-1 (Fig. 4a).

Fig. 4

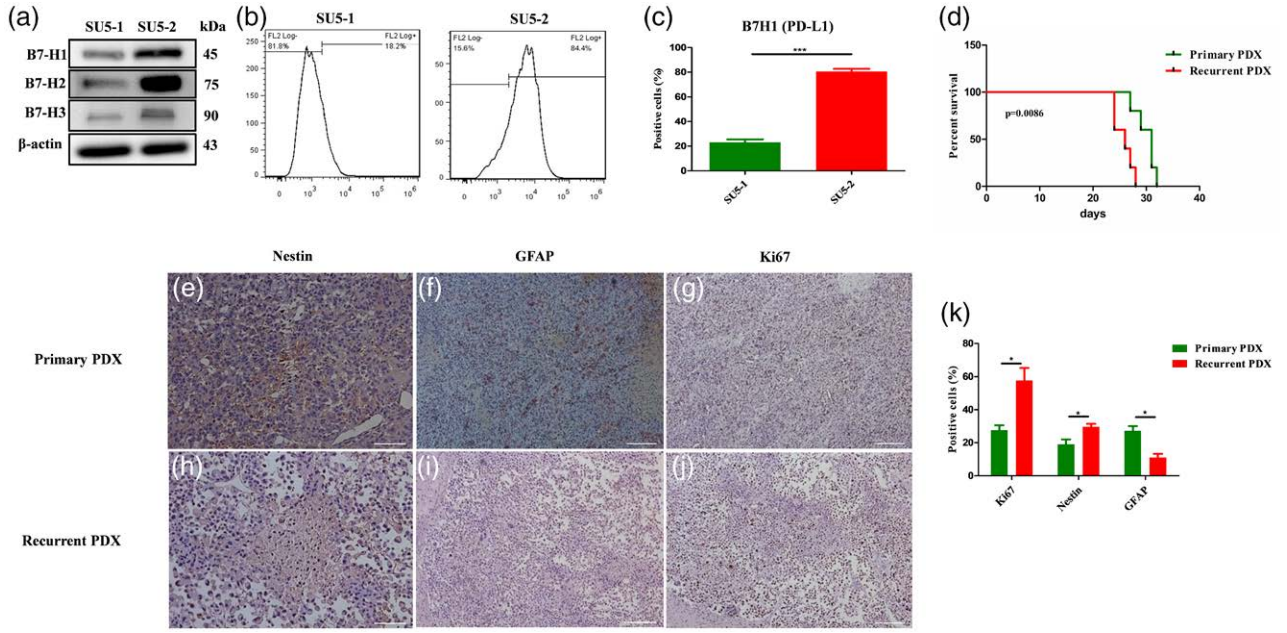

The expression of B7-H1 (PD-L1) was upregulated in SU5-2, and the OS of recurrent PDX model was worse. (a) Western blot analysis of B7-H1, B7-H2 and B7-H3 in SU5-1 and SU5-2. (b, c) Flow cytometry was applied to analyze the positive cells of B7-H1 (PD-L1) in SU5-1 and SU5-2. (d) The survival analysis of PDX models, Kaplan–Meier curve indicated the worse OS in the recurrent PDX model. (e–g, h–j). Immunohistochemical staining of Nestin, GFAP and Ki67 in primary and recurrent PDX models (×200). (k) Statistical analysis of the positive rate of Ki-67, Nestin and GFAP in primary and recurrent PDX models. *$P<0.05$, **$P<0.01$. GFAP, glial fibrillary acidic protein; OS, overall survival; PDX, patient-derived xenograft tumor.

Flow cytometry analysis also confirmed that the positive rate of B7-H1 (PD-L1) was higher in SU5-2 (Fig. 4b and c). These results might suggest that SU5-2 had a stronger inhibitory effect on T cell anti-tumor immunity.

PDX models of primary and recurrent glioblastoma

In vivo, the OS was used to evaluate the tumorigenicity and invasiveness of the tumor. We established PDX models of primary and recurrent glioblastoma in order to retain the original tumorigenic characteristics. The median survival of the primary PDX group was 31 days as the recurrent PDX group was 26 days. Kaplan–Meier survival curve analysis showed that the prognosis of recurrent PDX was worse ($P<0.05$) (Fig. 4d). In transplanted tumors, the GFAP and Nestin expression was consistent with the clinical glioblastoma samples (Fig. 4e, f, h, i and k). Moreover, Ki67 proliferation index was higher in the recurrent PDX, suggesting that recurrence glioblastoma had more proliferative activity (Fig. 4 G, J, K). Genetic analysis showed that the results of *EGFR* amplification, genes mutation of *IDH*, *Pten* and *PDGFRα*, *MGMT* methylation in the primary and recurrent PDX models were consistent with clinical glioblastoma specimens (Table 1).

Discussion

The molecular mechanism of glioblastoma occurrence, progression and the research of anti-tumor drugs have always been a hot spot in the field of neurotumor [18]. However, the tool cells commonly used have accumulated a lot of molecular genetic variations that are not related to original tumors. In addition, glioblastoma has a high degree of molecular genetics differences, which makes cell lines express different biomarkers [19]. In particular, the drug-resistant cell lines induced *in vitro* cannot faithfully retain the molecular characteristics of primary tumor. Therefore, the establishment of primary tumor cell lines with different characteristics will help us to further study the mechanism of glioblastoma recurrence and chemoresistance, providing a reliable platform for basic research, clinical translation and drug screening.

In this study, primary and recurrent glioblastoma specimens of the single patient were primarily cultured separately. During the course of the patient, tumor cells had no molecular genetic changes such as super progression caused by radiotherapy and chemotherapy pressure selection [20]. The natural recurrence of tumor depends on tissue remodeling initiated by tumor stem cells. Consequently, we established primary and recurrent GSCs lines, verified their differences in molecular genetics, and evaluated their stability in original glioblastoma specimens, *in vitro* and PDX models. The results suggested that the peculiarities of the original glioblastoma were still retained after primary culture *in vitro* and

transplantation *in vivo*. SU5-2 cells derived from recurrent glioblastoma had stronger proliferation, self-renewal and invasion capacity.

At present, the efficacy of chemotherapy for glioblastoma is limited [21], which is related to the difficulty of passing through the blood-brain barrier and the heterogeneity of glioblastoma leading to chemotherapy tolerance [22]. In this study, temozolomide, the first choice of chemotherapy for glioblastoma, was applied to primary and recurrent GSCs, respectively. We found that a low concentration of temozolomide had no obvious inhibitory effect on GSCs. Although this patient did not undergo chemotherapy screening, SU5-2 based on the recurrence specimen still showed higher tolerance to temozolomide than SU5-1. PD-1/PD-L1 has been the focus of tumor immunity [23]. Tumor cells overexpressing PD-1/PD-L1 have stronger chemotherapy tolerance [24], suggesting that the PD-1/PD-L1 pathway is not only related to antitumor immunity of tumor T cells [25], but also closely related to chemoresistance. However, the latter is rarely been involved in the study of glioblastoma. In order to explore the problem, we not only analyzed the expression of B7-H1 (PD-L1) in GSCs, but also detected B7-H2 and B7-H3 which also belong to B7 family of costimulatory molecules. The results showed that these proteins were upregulated in SU5-2. In addition to the role of the immune checkpoint, PD-1/PD-L1 may be a target molecule for chemotherapy sensitization and provide ideas for clinical treatment of glioblastoma.

High-frequency mutations are presented in 17% of recurrent glioblastoma samples treated with temozolomide, most of which come from genes encoding DNA mismatch repair proteins. These high-frequency mutations are consistent with the genetic phenotype of recurrent glioblastoma [26]. Glioblastoma in radiotherapy and chemotherapy can be regarded as an evolutionary process of continuous replacement of cell clones. In this study, the primary culture of glioblastoma without chemoradiotherapy was carried out, and the GSCs lines and PDX models were established as well. It was helpful to observe the natural properties of GSCs and compare molecular biological characteristics changes. However, due to the failure to obtain normal tissue samples from patients, it was difficult to compare the molecular differences between primary and recurrent glioblastoma in the follow-up genome-wide analysis, so only limited target molecular changes could be analyzed.

With the advancement of cell culture technology, the primary cell model and corresponding PDX model derived from patients' surgical specimens can faithfully replicate the molecular genetic characteristics of original tumors, which provide a stable, reliable, and sufficient experimental platform for research on tumor-related properties and screening of clinical drug targets.

Conclusion

In this study, we compared the biological differences of the primary and recurrent GSCs from the single glioblastoma patient at both in-vivo and in-vitro levels. Compared with our previous report [27], which described ectopic tumor recurrence after postoperative radio-chemotherapy with no difference in genetic changes between the primary and recurrent GSCs. We showed a case of glioblastoma patient with spontaneous recurrence *in situ*, the corresponding molecular analysis is free of the interference of radio- or chemotherapy-induced hyperprogression of glioblastoma. Besides, we not only established PDX model to reproduce the tumorigenic characteristics of glioblastoma in vivo but also established primary and recurrent GSCs lines by brief primary cell culture, which could reflect the individualized characteristics and were conducive to the subsequent individualized treatment of glioblastoma.

Acknowledgements

The study was funded by Natural Science Foundation of Jiangsu Province (grant no. BK20201172); Clinical Special Disease Diagnosis and Treatment Technology in Suzhou (grant no. LCZX201807); Key project of Jiangsu Health Commission (ZDB2020016); Young Talent Development Plan of Changzhou Health Commission (grant no. 2020-233-CZQM2020013) and Major Science and Technology Project of Changzhou Municipal Health Commission (ZD202005).

J.S. was a major contributor to molecular experiments and article writing. X.C.D. and W.H. performed statistical analysis of the experimental data. P.Z., L.L. and H.Y.W. cultured cells and in-vitro experiments. Q.Q.J. and H.R.L. were involved in a review of the article. S.C. and S.W.L. were patient management and sample collection. J.Q.Y. and Z.Y.Q. were responsible for animal feeding and tumorigenicity experiments. J.D. was responsible for the design and supervision of the experiments. All authors read and approved the final article.

Procedures performed in the study were in accordance with the ethical standards of the institutional research committee.

This study was approved by the ethics committee of the Second Affiliated Hospital of Soochow University.

The datasets are available from the corresponding author on reasonable request.

Conflicts of interest

There are no conflicts of interest.

References

1 Xue S, Song G, Yu J. The prognostic significance of PD-L1 expression in patients with glioma: a meta-analysis. *Sci Rep* 2017; **7**:4231.

2 Kurz SC, Cabrera LP, Hastie D, Huang R, Unadkat P, Rinne M, *et al.* PD-1 inhibition has only limited clinical benefit in patients with recurrent high-grade glioma. *Neurology* 2018; **91**:e1355–e1359.

3 Allen M, Bjerke M, Edlund H, Nelander S, Westermark B. Origin of the U87MG glioma cell line: good news and bad news. *Sci Transl Med* 2016; **8**:354re3.
4 Reardon S. US science agencies face budget limbo. *Nature* 2016; **537**:149.
5 He J, Liu Y, Lubman DM. Targeting glioblastoma stem cells: cell surface markers. *Curr Med Chem* 2012; **19**:6050–6055.
6 Zhou BB, Zhang H, Damelin M, Geles KG, Grindley JC, Dirks PB. Tumour-initiating cells: challenges and opportunities for anticancer drug discovery. *Nat Rev Drug Discov* 2009; **8**:806–823.
7 Sun C, Dai X, Zhao D, Wang H, Rong X, Huang Q, Lan Q. Mesenchymal stem cells promote glioma neovascularization *in vivo* by fusing with cancer stem cells. *BMC Cancer* 2019; **19**:1240.
8 Buccarelli M, Marconi M, Pacioni S, De Pascalis I, D'Alessandris QG, Martini M, *et al*. Inhibition of autophagy increases susceptibility of glioblastoma stem cells to temozolomide by igniting ferroptosis. *Cell Death Dis* 2018; **9**:841.
9 Galavotti S, Bartesaghi S, Faccenda D, Shaked-Rabi M, Sanzone S, McEvoy A, *et al*. The autophagy-associated factors DRAM1 and p62 regulate cell migration and invasion in glioblastoma stem cells. *Oncogene* 2013; **32**:699–712.
10 Fei XF, Zhang QB, Dong J, Diao Y, Wang ZM, Li RJ, *et al*. Development of clinically relevant orthotopic xenograft mouse model of metastatic lung cancer and glioblastoma through surgical tumor tissues injection with trocar. *J Exp Clin Cancer Res* 2010; **29**:84.
11 Han B, Meng X, Wu P, Li Z, Li S, Zhang Y, *et al*. ATRX/EZH2 complex epigenetically regulates FADD/PARP1 axis, contributing to TMZ resistance in glioma. *Theranostics* 2020; **10**:3351–3365.
12 Tao Z, Li T, Ma H, Yang Y, Zhang C, Hai L, *et al*. Autophagy suppresses self-renewal ability and tumorigenicity of glioma-initiating cells and promotes Notch1 degradation. *Cell Death Dis* 2018; **9**:1063.
13 Reardon DA, Nabors LB, Mason WP, Perry JR, Shapiro W, Kavan P, *et al*.; BI 1200 36 Trial Group and the Canadian Brain Tumour Consortium. Phase I/randomized phase II study of afatinib, an irreversible ErbB family blocker, with or without protracted temozolomide in adults with recurrent glioblastoma. *Neuro Oncol* 2015; **17**:430–439.
14 Guo G, Gong K, Puliyappadamba VT, Panchani N, Pan E, Mukherjee B, *et al*. Efficacy of EGFR plus TNF inhibition in a preclinical model of temozolomide-resistant glioblastoma. *Neuro Oncol* 2019; **21**:1529–1539.
15 Vengoji R, Macha MA, Nimmakayala RK, Rachagani S, Siddiqui JA, Mallya K, *et al*. Afatinib and temozolomide combination inhibits tumorigenesis by targeting EGFRvIII-cMet signaling in glioblastoma cells. *J Exp Clin Cancer Res* 2019; **38**:266.
16 Barbarisi M, Barbarisi A, De Sena G, Armenia E, Aurilio C, Libutti M, *et al*. Boswellic acid has anti-inflammatory effects and enhances the anticancer activities of temozolomide and afatinib, an irreversible ErbB family blocker, in human glioblastoma cells. *Phytother Res* 2019; **33**:1670–1682.
17 Wang Z, Zhang C, Liu X, Wang Z, Sun L, Li G, *et al*. Molecular and clinical characterization of PD-L1 expression at transcriptional level via 976 samples of brain glioma. *Oncoimmunology* 2016; **5**:e1196310.
18 Shankar GM, Kirtane AR, Miller JJ, Mazdiyasni H, Rogner J, Tai T, *et al*. Genotype-targeted local therapy of glioma. *Proc Natl Acad Sci USA* 2018; **115**:E8388–E8394.
19 Diaz AK, Baker SJ. The genetic signatures of pediatric high-grade glioma: no longer a one-act play. *Semin Radiat Oncol* 2014; **24**:240–247.
20 López GY, Van Ziffle J, Onodera C, Grenert JP, Yeh I, Bastian BC, *et al*. The genetic landscape of gliomas arising after therapeutic radiation. *Acta Neuropathol* 2019; **137**:139–150.
21 Koshkin PA, Chistiakov DA, Chekhonin VP. Role of microRNAs in mechanisms of glioblastoma resistance to radio- and chemotherapy. *Biochemistry (Mosc)* 2013; **78**:325–334.
22 Baker GJ, Yadav VN, Motsch S, Koschmann C, Calinescu AA, Mineharu Y, *et al*. Mechanisms of glioma formation: iterative perivascular glioma growth and invasion leads to tumor progression, VEGF-independent vascularization, and resistance to antiangiogenic therapy. *Neoplasia* 2014; **16**:543–561.
23 Zhang J, Bu X, Wang H, Zhu Y, Geng Y, Nihira NT, *et al*. Cyclin D-CDK4 kinase destabilizes PD-L1 via cullin 3-SPOP to control cancer immune surveillance. *Nature* 2018; **553**:91–95.
24 Ishibashi M, Tamura H, Sunakawa M, Kondo-Onodera A, Okuyama N, Hamada Y, *et al*. Myeloma drug resistance induced by binding of myeloma B7-H1 (PD-L1) to PD-1. *Cancer Immunol Res* 2016; **4**:779–788.
25 McClanahan F, Riches JC, Miller S, Day WP, Kotsiou E, Neuberg D, *et al*. Mechanisms of PD-L1/PD-1-mediated CD8 T-cell dysfunction in the context of aging-related immune defects in the Eμ-TCL1 CLL mouse model. *Blood* 2015; **126**:212–221.
26 Wang J, Cazzato E, Ladewig E, Frattini V, Rosenbloom DI, Zairis S, *et al*. Clonal evolution of glioblastoma under therapy. *Nat Genet* 2016; **48**:768–776.
27 Huang Q, Zhang QB, Dong J, Wu YY, Shen YT, Zhao YD, *et al*. Glioma stem cells are more aggressive in recurrent tumors with malignant progression than in the primary tumor, and both can be maintained long-term *in vitro*. *BMC Cancer* 2008; **8**:304.